

Title : will be set by the publisher
Editors : will be set by the publisher
EAS Publications Series, Vol. ?, 2019

NEWAGE

Kentaro Miuchi¹, Kiseki Nakamura¹, Atsushi Takada¹, Satoshi Iwaki¹,
 Hidetoshi Kubo¹, Tetsuya Mizumoto¹, Hironobu Nishimura¹,
 Joseph Parker¹, Tatsuya Sawano¹, Toru Tanimori¹, Hiroyuki Sekiya²,
 Atsushi Takeda², Takahiro Fusayasu³, Akira Sugiyama⁴ and Manobu
 Tanaka⁵

Abstract. NEWAGE is a direction-sensitive dark matter search experiment with a gaseous time-projection chamber. We improved the direction-sensitive dark matter limits by our underground measurement. After the first underground run, we replaced the detector components with radio-pure materials. We also studied the possibilities of head-tail recognition of nuclear tracks in the surface laboratory. For the future large volume detector, we are developing a pixel ASIC named QPIX. In this paper, these recent R&D activities are described.

1 Introduction

Direction-sensitive dark matter search with gaseous detector was proposed in late 1980s (Rich and Spiro, 1988; G. Masek et al., 1989; G. Gerbier et al., 1989). Since then several experimental and theoretical works on the possibility of detecting this distinct signal of dark matter have been performed (A. M. Green and B. Morgan, 2007; P. Belli et al., 1992; R. Bernabei et al., 2003; H. Sekiya et al., 2004; K. N. Buckland et al., 1994; Tanimori et al., 2004; Dujmic et al., 2008; T. Naka et al., 2007; MIMAC, 2011). Among these proposed methods, The DRIFT group has pioneered studies of gaseous detectors for WIMP-wind detection for more than ten years with multi-wire proportional chambers (Burgos et al., 2009).

¹ Cosmic-Ray Group, Department of Physics, Graduate School of Science, Kyoto University
 Kitashirakawa-oiwakecho, Sakyo-ku, Kyoto, 606-8502, Japan e-mail: miuchi@cr.scphys.kyoto-u.ac.jp

² Kamioka Observatory, ICRR, The University of Tokyo Higashi-Mozumi, Kamioka cho,
 Hida 506-1205 Japan

³ Nagasaki Institute of Applied Science, Nagasaki, Japan

⁴ Saga University, Saga, Japan

⁵ Institute of Particle and Nuclear Studies, KEK, Tsukuba, Japan

name	μ -PIC	drift	location	use
NEWAGE-0.1a	$10 \times 10\text{cm}^2$	10 cm	surface	advanced test
NEWAGE-0.3a	$30 \times 30\text{cm}^2$	30 cm	underground	DM run, BG study
NEWAGE-0.3b	$30 \times 30\text{cm}^2$	50 cm	surface	large volume

Table 1. Specifications of NEWAGE TPCs.

name	volume	PIN detector
NEWAGE-RD1	22.5diameter \times 15cm	HPK S3590-02
NEWAGE-RD2	22.3diameter \times 10cm	HPK S3590-09

Table 2. Specifications of NEWAGE radon detectors.

We started a new project, New generation WIMP-search with Advanced Gaseous tracking device Experiment (NEWAGE) in 2003(Tanimori et al., 2004). We adopted a new technology named Micro-Patterned Gaseous Detector (MPGD) and thus had advantages in the pitch of the detection sensors and a three-dimensional tracking scheme. We performed first direction-sensitive dark matter search experiment in a surface laboratory (Miuchi et al., 2007) and updated the direction-sensitive limits by the measurement in an underground laboratory(Miuchi et al., 2010). Although we set a WIMP-proton cross section of 5400 pb for 150 GeV WIMPs by a direction-sensitive methods, we need to improve more than three orders of magnitude to set a competitive limits to other direction-insensitive searches. We plan to improve the sensitivity by reducing the internal radioactive background, lowering the energy threshold, discriminating head-tails of nuclear tracks, building large-volume detectors, and developing the pixel readout. In this paper, we report these efforts after our first underground run.

2 NEWAGE detectors

We have three time projection chambers (TPCs) and two Radon Detectors. We list the specifications of our TPCs in Table 1. We have one large TPC in the underground laboratory for dark matter run and background studies. We have one large and one small TPC in the surface laboratory for mainly large volume R&D and advanced tests, respectively. We use μ -PIC(Ochi et al., 2001; Takada et al., 2007), one of the micro patterned gaseous detector, as a main-multiplier and a readout of the TPC. The pitch of the μ -PIC is 400 μm . We also use gas an electron multiplier (GEM)(Sauli and Sharma, 1999) as a sub-multiplier. A typical schematic view of our TPC is shown in Fig. 1. For details on our TPC system, please refer to our previous publication(Miuchi et al., 2010) and the references therein. We developed electrostatic collection radon detectors similar to the system developed by the Super-Kamiokande group(Y Takeuchi and others, 1999). We operate the radon detector with the CF_4 at 152 Torr to measure the radon emanation into the TPC gas. Specifications of our radon detectors are shown in Table 1.

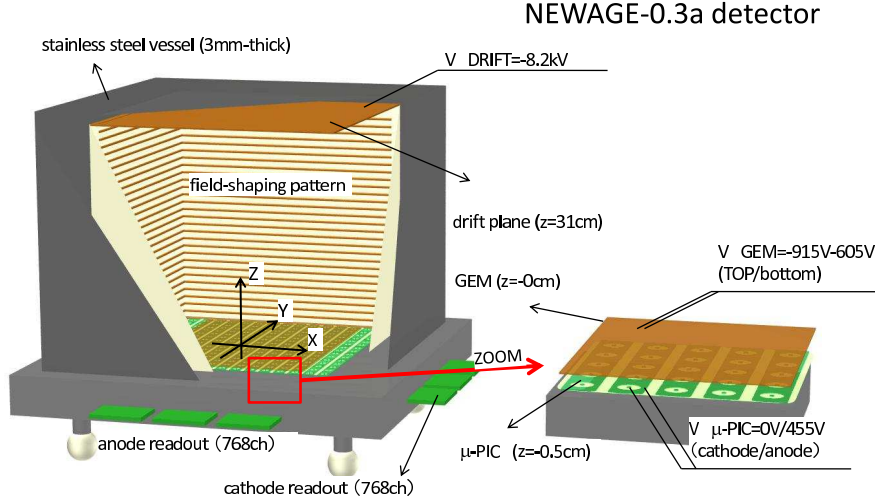


Fig. 1. Schematic view of NEWAGE-0.3a detector. The volume between the drift plane and the GEM is the detection volume, it is filled with CF_4 gas at 152 Torr.

3 Underground R & D

One of the major background in our detector is radons coming from uranium and thorium contaminations in the detector materials.

3.1 Radon elimination system

We attached a mini-chamber containing about 100 gram of charcoal (TSURUMI-COAL 2GS) as radon filter and circulated the TPC gas with a Teflon bellows pump (TSURUMICOAL 2GS). With this radon elimination system, radon rate was decreased to less than 1/10.

3.2 Material selection and detector update

We measured the radon emanation from main components of our detector with our radon detectors. As the absolute detection efficiency of the radon-daughter ion was not measured yet, we relatively compared the contribution of each components. Measured results normalized to the NEWAGE-0.3a detector is shown in Figure 3. We found the glass-reinforced fluoroplastic (TPC cage) had the largest radon

material	radon rate per NEWAGE-0.3a (a.u.)
glass-reinforced fluoroplastic (TPC cage)	1
PTFE (TPC cage)	$0.1 >$
glass-reinforced plastic (GEM frame)	$0.7 \times 10^{-2} >$
polyimide+copper (GEM)	$0.1 >$
resistors (TPC)	$0.8 \times 10^{-2} >$
μ -PIC	$0.1 >$

Table 3. Relative contribution of the detector components to the radon background.

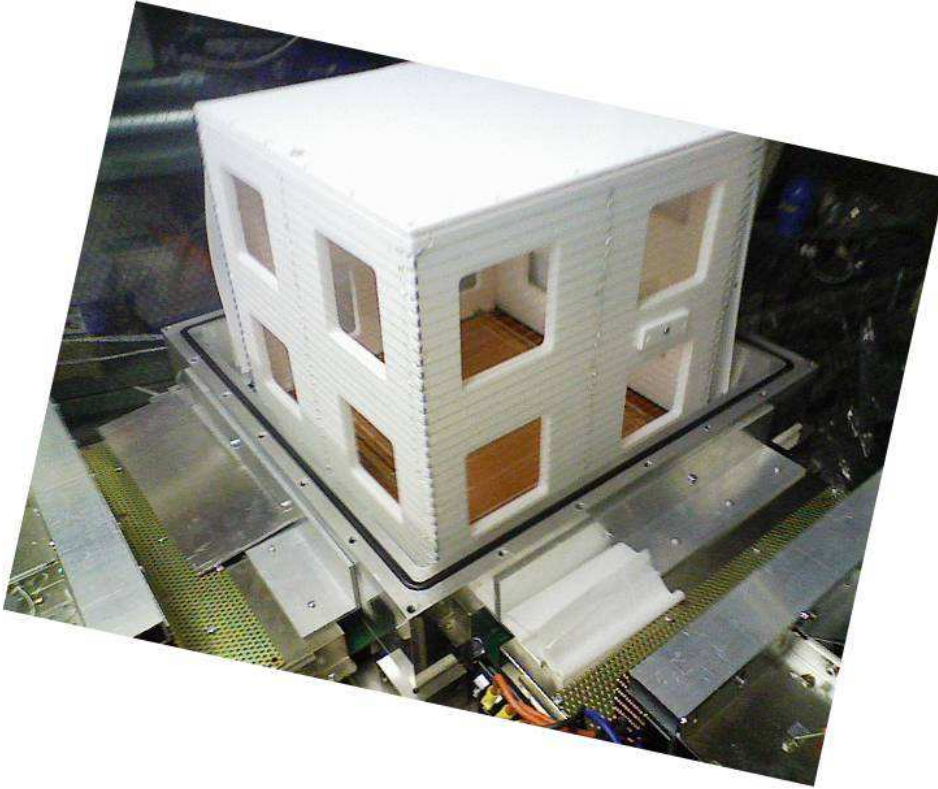


Fig. 2. Picture of NEWAGE-0.3a detector with a new drift cage made of PTFE.

emanation. We decided to replace it with PTFE. The picture of our new TPC cage is shown in Fig. fig:PTFE-TPC. The radon background is now expected to be less than $1/3$. With these major and minor improvements, we started a dark matter run on August 3rd, 2011.

run	70-100keV	100-200keV	200-400keV
+X	8608	7389	9607
-X	7301	5842	6489
+Y	6751	4857	4486
-Y	3926	2967	2701
total	26586	21055	23283

Table 4. Number of events used for analysis in each run. Note that the four spectrum shapes are not same due to the asymmetry of the TPC cage.

4 Surface R & D

4.1 Head-tail recognition

Head-tail recognition of the nuclear track is important to improve the sensitivity of a direction-sensitive dark matter search experiment (A. M. Green and B. Morgan, 2007). DM-TPC group has shown the possibility of head-tail recognition of high energy nuclear tracks (D. Dujmic et al., 2008) followed by the DRIFT group's work in the energy range relevant to the dark matter search for one dimension (S. Burgos and others, 2009).

We updated the FPGA firmware of our DAQ system in order to study the two-dimensional head-tail recognition with the NEWAGE-0.1a detector. We used to take X-Y coincidence in the FPGA at the rise of each hit. We modified the firmware so that we do not require X-Y coincidence but record the rising and falling edges of all of the hit-strips (TPC-mode5). We show a typical nuclear recoil event in Fig. 3. The energy is about 130 keV¹.

We defined a skewness γ_{x_i} along $x_i = (x, y)$ axis by equation 4.1, where $q(x_i)$ is the pulse duration at x_i and $\langle x_i \rangle$ is the mean value of x_i with $q(x_i) > 0$.

$$\gamma_{x_i} = \frac{\langle (q(x_i) \cdot (x_i - \langle x_i \rangle)^3) \rangle}{\langle (q(x_i) \cdot (x_i - \langle x_i \rangle)^2)^{3/2} \rangle} \quad (4.1)$$

We measured the skewness by placing a ²⁵²Cf neutron source at four positions, (30cm, 0cm, 5cm) (+X run), (-30cm, 0cm, 5cm) (-X run), (0cm, 30cm, 5cm) (+Y run), and (0cm, -30cm, 5cm) (-Y run). See Fig. 1 for the coordinates. Number of events used for the analysis is shown in Table 4. Skewness distributions of +X run and -X run are shown in Fig. 4. We fitted the distributions with a Gaussian function and we indicate the center value and its fitting errors in the figure. The difference between the center values of +X and -X runs are statistically significant, while the center values of +Y run and -Y runs are statistically consistent.

We show the energy dependence of γ_x and γ_y in Fig. 5 and Fig. 6, respectively. Though the statistics are not enough, positive (negative) skewness were observed in the +X (-X) and +Y (-Y) runs.

¹We calibrated the detector with alpha particle of about 1.5 MeV, so we use an alpha-equivalent energy in this paper.

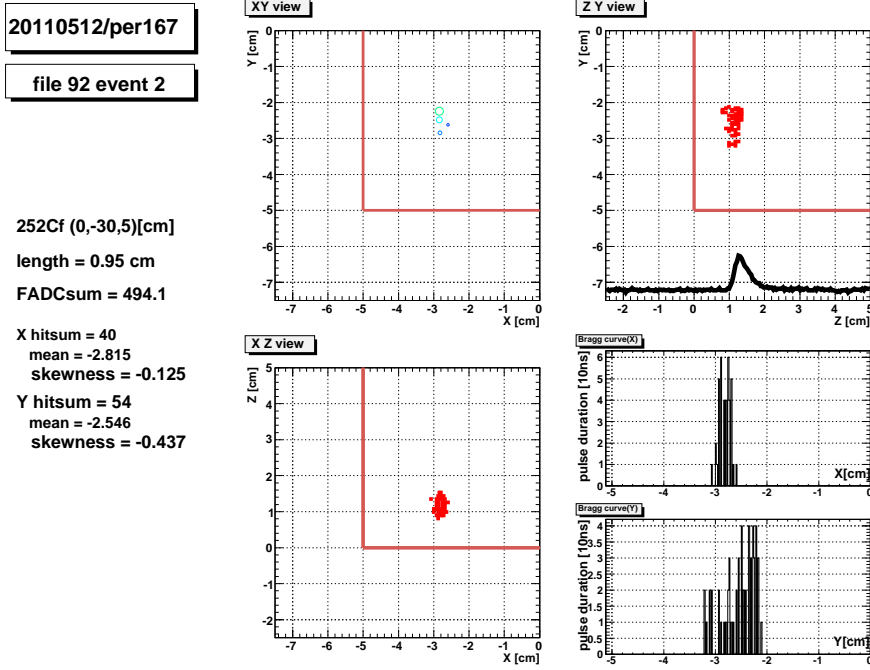


Fig. 3. Typical event recorded with a improved DAQ system (TPC-mode5). One set of raw data is a group of (X,Z) or (Y,Z) and is shown with red square marks in the right-top and left-bottom panels. The pulse duration (time-over-threshold, TOT) at each strip is counted from the raw@data and we plot them as a function of each coordinate in the right-bottom panels. TOT have correlation with the charge. With a software coincidence, X-Y track image is made, which is shown with open circles in the left-top panel. A size of each mark indicates the pulse duration of a coincidence hit. The energy is 130keV.

We then combined these results into parallel(γ_x in $\pm X$ runs and γ_y in $\pm Y$) data and orthogonal(γ_y in $\pm X$ runs and γ_x in $\pm Y$) data. In the parallel runs, absolute values of the skewness are used.. The result is shown in Fig. 7. In the parallel runs, statically significant γ with 3.0σ , 3.9σ , and 7.7σ are observed for the energy range of 70-100keV, 100-200keV, and 200-400keV, respectively. The γ were consistent with zero in the orthogonal runs.

Although the skewness definition is not optimized, these results shows that we can recognize head-tail with a sufficient statistics down to 70 keV. These results also indicate much more efforts required for event-by-event recognition.

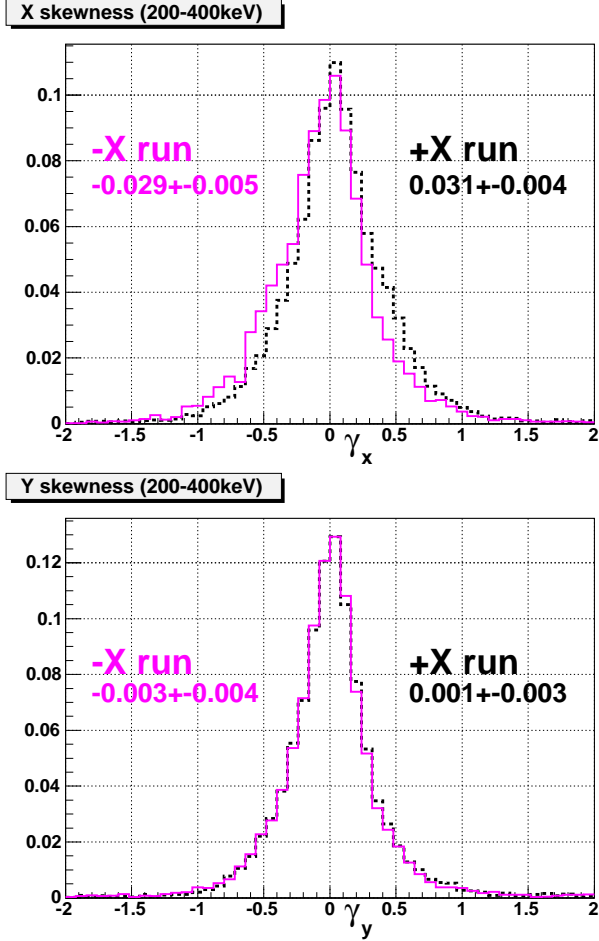


Fig. 4. Skewness distributions of +X run and -X run. The top and bottom panel shows the skewness along X axis (γ_x) and Y (γ_y) axis, respectively. The energy range is 200 - 400 keV. The center value of a Gaussian function and its fitting errors are indicated. The difference between the center values of +X and -X runs are statistically significant, while the center values of +Y run and -Y runs are statistically consistent.

5 R&D for pixel-readout TPC

5.1 Pixel readout TPC

TPCs for direction-sensitive dark matter search experiments need to detect short ($\sim 1\text{mm}$) tracks with a reasonable ($\sim 30^\circ$) angular resolution. Most of these experiments use strip or MWPC readout (DRIFT, 2011; MIMAC, 2011; NEWAGE, 2011), mostly because of the technical limitations. We are confronted with tracking diffi-

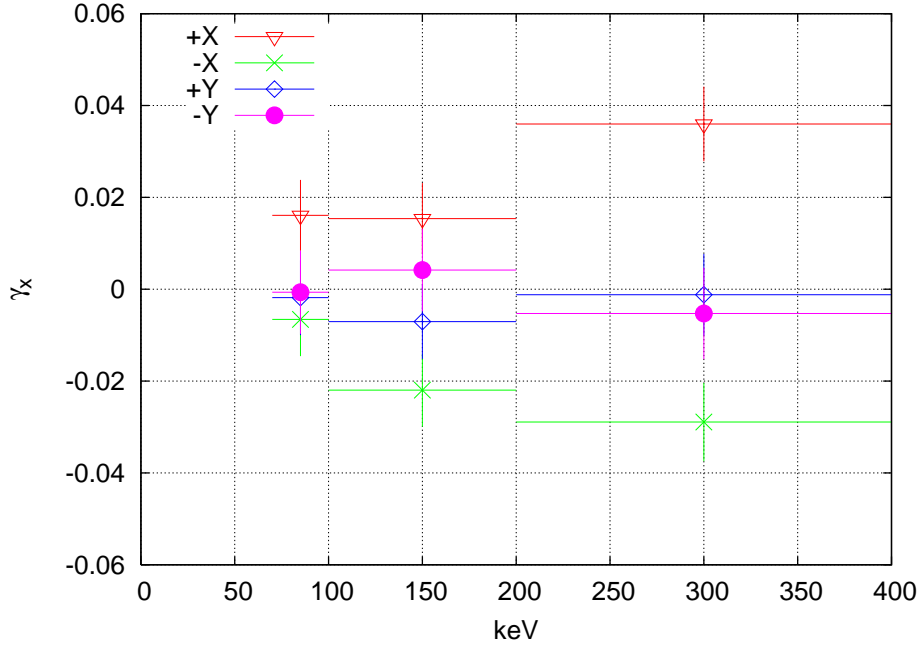


Fig. 5. Energy dependence of γ_x . Triangle (red online), cross (green), diamond (blue) and circle (violet) shows +X, -X, +Y, and -Y runs, respectively.

culties such as double-hit unfolding problems. And thus none of us has achieved a required tracking performance with existing readout systems. A pixel-readout is an ideal solutions to these tracking difficulties and would bring a breakthrough to this field. Pixel-readout TPCs would realize the detection of the three-dimensional distribution of primary electrons, and thus we can in principle reconstruct the nuclear track without losing any information at the readout stage. With these undeteriorated data, a better angular resolution with a good direction uniformity is expected. A better head-tail recognition is also expected. There are several achievements in the world to develop ASICs (application specified integrated circuits) for pixel readout TPCs. TIMEPIX(Llopart et al., 2007), developed in CERN, is a well known PIXEL-readout ASIC which measures the time-of-flight (TOF) and the time-over-threshold (TOT) with a pitch of $55 \mu\text{m}$. TOT is a good parameter to estimate collected charge as long as the longitudinal diffusion is small. A dark matter detector needs to be as large as possible for a given detection area, and thus we want to have the drift region as long as possible. Then the longitudinal diffusion cannot be ignored and TOT no longer helps. If we can have an ADC function in each pixel, though this is not very easy, this problem should be solved. We can, furthermore use the ADC-TOT correlation to estimate the absolute z position. Absolute z, even if the resolution is several cm, would greatly help to

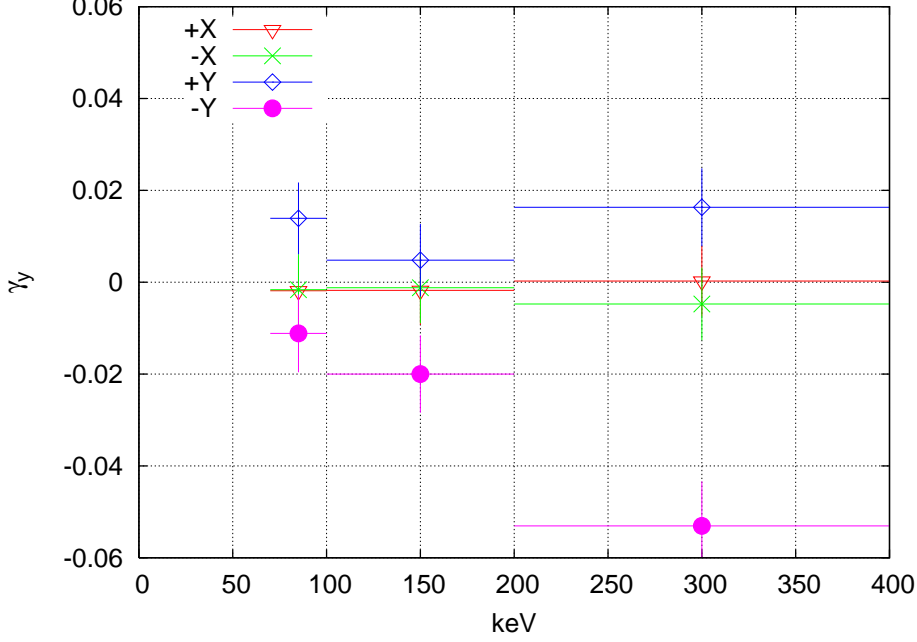


Fig. 6. Energy dependence of γ_y . Triangle (red online), cross (green), diamond (blue) and circle (violet) shows +X, -X, +Y, and -Y runs, respectively.

reduce the radioactive background from the drift plane, the GEM, and the μ -PIC.

We are developing a CMOS ASIC named QPIX which has ADC in addition to TOF and TOT in each pixel (KHOA, 2010). This development is in a starting phase and we are making efforts to prove the principle of concept and also evaluate the cost and background of the readout system.

5.2 QPIX-ver1

After the R&D with several types of TEGs (test element groups) we developed QPIX-ver1, which is a first version with two-dimensional array. The design values of QPIX-ver1 are shown in Table 5 together with a goal values. QPIX-ver1 has 20×20 pixels with a pitch of $200 \mu\text{m}$. Each pixel has 14-bit TOF, 8-bit TOT, and 10 bit ADC. The chip was made by TSMC $0.18 \mu\text{m}$ process. A microscope photo is shown in Fig. 8. 20×20 pixels are seen. 84 IO pads are placed along three edges of the chip. The inset shows the zoom-up of one pixel. A metal pad area is indicated by dashed line. We can use this pad area for the direct charge collection from the gas volume or for the contact pad of bump bonding. A trace of bump bonding test is seen in the center. The circuit area is $130 \times 130 \mu\text{m}^2$.

We tried two ways of mountings, namely a wire-bonding mounting and a flip-chip mounting. Both mounting ways are shown in Fig 9. Wire-bonding methods

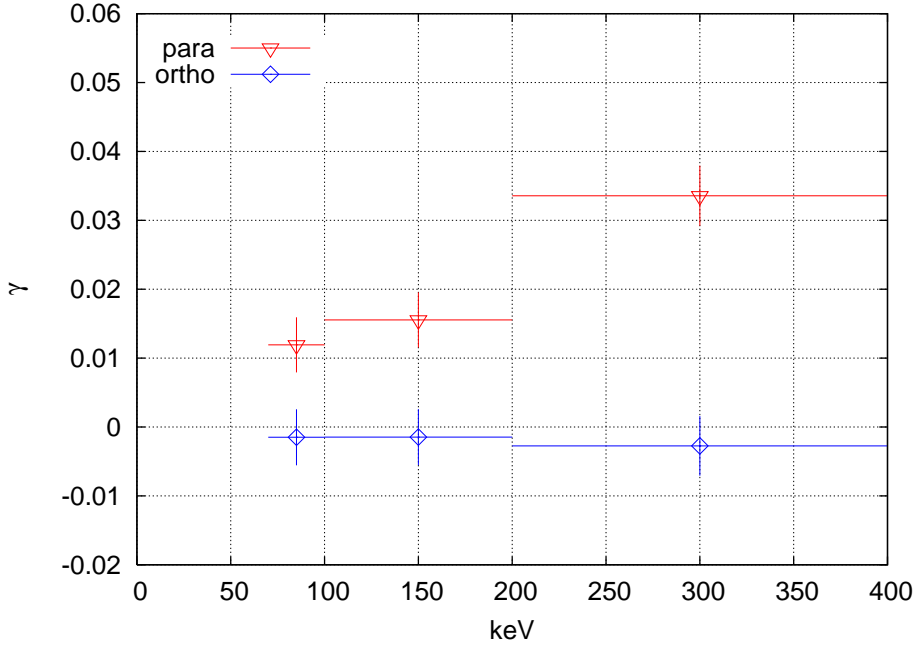


Fig. 7. Energy dependence of the combined skewness. The triangle (red online) and diamond (blue) show the skewness parallel and orthogonal to the incoming neutrons. Only statistical errors are considered.

	QPIX-ver1 (design)	QPIX goal
dimension	$200 \times 200 \mu\text{m}^2$	$200 \times 200 \mu\text{m}^2$
channels	$20 \times 20 \text{ch/chip}$	
TOF	14 bits	14bits
TOT	8 bits	8bits
comparator threshold(TOF,TOT)	10fC	1fC
clock(TOT,TOT)	100MHz	100MHz
ADC	1.5pC / 10bits, 10Msps	100fC / 10bits, 10Msps

Table 5. Design values of QPIX-ver1. The goal values are also shown.

is shown in the left panel. This is a well-studied and very reliable method. We use wire-bondings to connect the IO pads of QPIX-ver1 to the readout PCB. The problem of the wire-bonding method is dead areas. We have dead areas at least along one edge with wire-bonding mountings.

We tried another method, flip-chip mounting, in order to decrease the dead areas. This method is shown in the right panel of Fig. 9. We mount a charge collection PCB(CCPCB) on QPIX-ver1 by bump bonding. The CCPCB has 20×20 pads on the gas side. These pads are connected to the cavity underneath

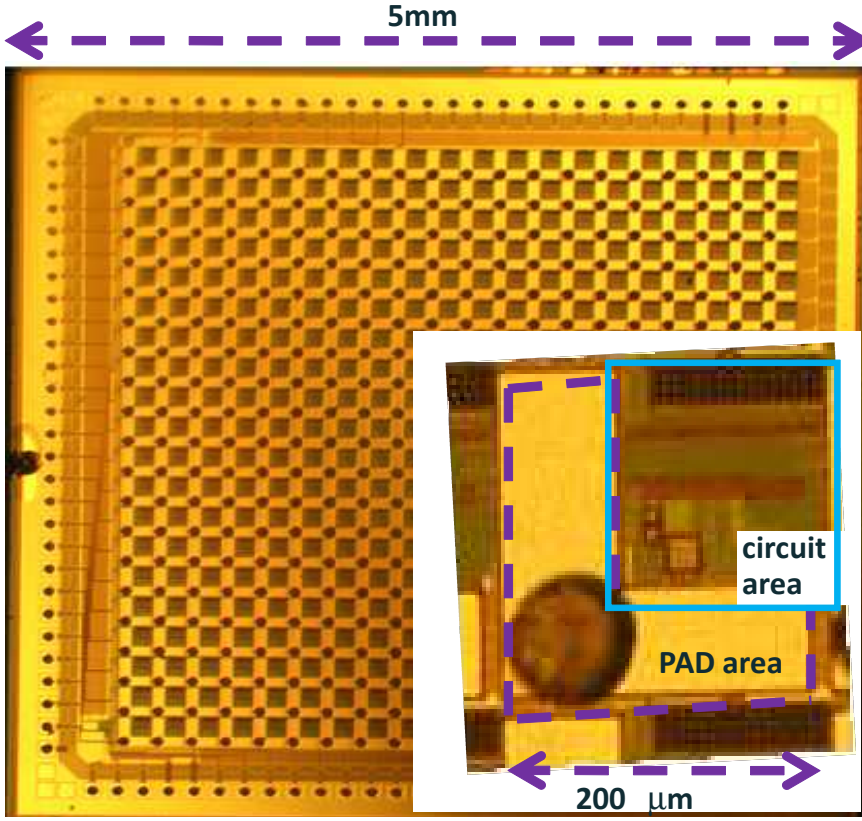


Fig. 8. A microscope photo of QPIX-ver1. 20×20 pixels are seen. The inset shows a zoom-up of one pixel.

through the CCPCB. QPIX-ver1 is mounted in this cavity by bump-bonding. IO pad are also connected by bump-bonding and are connected to the mother broad PCB(MBPCB) through CCPCB. The CCPCB is larger than QPIX-ver1 and can be mounted on a MBPCB without dead areas. We mounted four CCPCBs on a MBPCB. The picture of mounting is shown in Fig. 10. A mechanical mounting was confirmed, though electrical connection was not achieved. This was because the surface of the CCPCB cavity was not flat enough for the bump bonding. We are trying to produce a better CCPCB to establish the flip-chip mounting. We measured some performance of QPIX-ver1 mounted with the wire-bondings.

Measured performance of QPIX-ver1 is shown in Fig. 11. Four QPIX chips are mounted. Three chips worked, the rest had some trouble either in the ASIC development process or mounting process. TOF shows good linearity up to $2\mu s$. ADC shows fair linearity up to $1.5pC$ though the threshold was about ten times higher than the designed value. We are designing next TEG to improve the threshold.

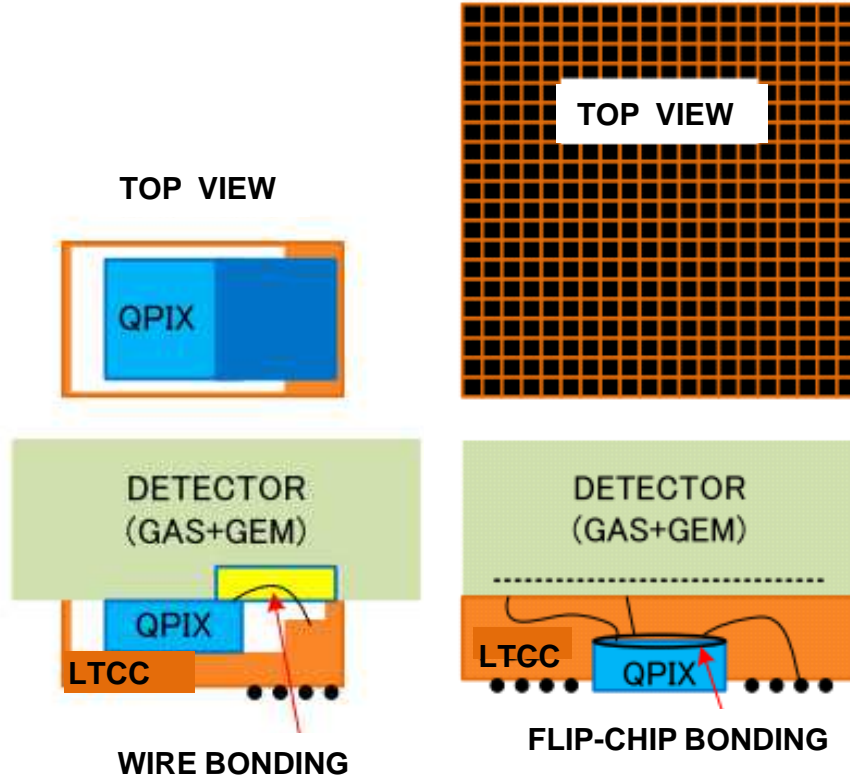


Fig. 9. Two ways of QPIX mounting. The left panel shows a wire-bonding mounting and the right shows a flip-chip mounting.

6 Conclusions

Intensive studies to improve the sensitivities of NEWAGE dark matter detectors are under way. We replaced the TPC cage with radio-pure PTFE. We expect at least five times less count rate due to the radioactive background from the detector components. We also studied the head-tail recognition in the surface laboratory using two-dimensional track data. Although the skewness definition is not optimized, these results show that we can recognize head-tail with a sufficient statistics down to 70 keV. These results also indicate much more efforts required for event-by-event recognition. For the future large volume detector, we are developing a pixel ASIC named QPIX. We made a first version of arrayed pixels and tried two ways of mountings methods. We started a new dark matter run in August 2010 expecting a better limits.

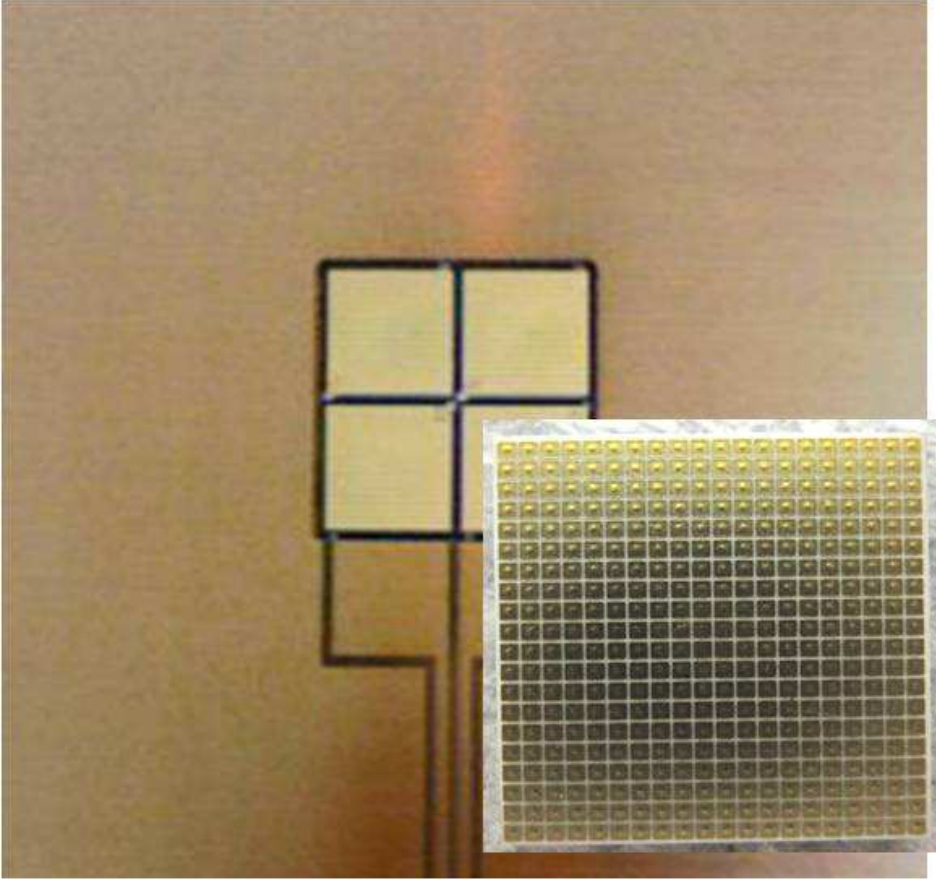


Fig. 10. Four CCPCBs are mounted on a MBPCB. Inset shows a zoom-up of a CCPCB.

Acknowledgments

This work was partially supported by KAKENHI Grant-in-Aids for Young Scientist(A) (19684005 and 23684014); KAKENHI Grant-in-Aids for Scientific Research(B) (21340063); KAKENHI Grant-in-Aids for Challenging Exploratory Research (23654084); KAKENHI Grant-in-Aids for JSPS Fellows; and Global COE Program “The Next Generation of Physics, Spun from Universality and Emergence” from the Ministry of Education, Culture, Sports, Science and Technology (MEXT) of Japan.

References

A. M. Green and B. Morgan: 2007, *Astropart. Phys.* **27**, 142

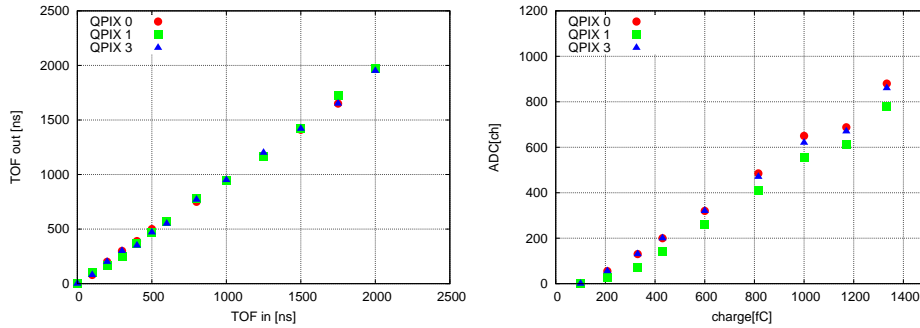


Fig. 11. Four CCPCBs are mounted on a MBPCB. Inset shows a zoom-up of a CCPCB.

- Burgos, H. et al.: 2009, *Nucl. Instrum. Methods Phys. Res. Sect. A* **600**, 417
D. Dujmic et al.: 2008, *Nucl. Instrum. Methods Phys. Res. Sect. A* **584**, 327
DRIFT: 2011, *these proceedings*
Dujmic, D. et al.: 2008, *Astropart. Phys.* **30**, 58
G. Gerbier et al.: 1989, *Proceedings of the Workshop on Particle Astrophysics* p. 43
G. Masek et al.: 1989, *Proceedings of the Workshop on Particle Astrophysics* p. 43
H. Sekiya et.al: 2004, *Proceedings of Fifth International Workshop on the Identification of Dark Matter* p. 378
K. N. Buckland et al.: 1994, *Phys. Rev. Lett.* **73**, 1067
KHOA, V. M.: February 2010, *Master Thesis* Tokyo Institute of Technology
Llopart, X., Ballabriga, R., Campbell, M., Tlustos, L., and Wong, W.: 2007, *Nucl. Instrum. Methods Phys. Res. Sect. A* **581**, 485
MIMAC: 2011, *these proceedings*
Miuchi, K. et al.: 2007, *Phys. Lett. B* **654**, 58
Miuchi, K. et al.: 2010, *Phys. Lett. B* **686**, 11
NEWAGE: 2011, *these proceedings*
Ochi, A. et al.: 2001, *Nucl. Instrum. Methods Phys. Res. Sect. A* **471**, 264
P. Belli et.al: 1992, *Nuovo Cimento C* **15**, 473
R. Bernabei et.al: 2003, *Eur. Phys. C* **28**, 203
Rich, J. and Spiro, M.: 1988, *Saclay preprint DPhPE 88-04*
S. Burgos and others: 2009, *Astropart. Phys.* **261**, 266
Sauli, F. and Sharma, A.: 1999, *Annu. Rev. Nucl. Part. Sci* **49**, 341
T. Naka et al.: 2007, *Nucl. Instrum. Methods Phys. Res. Sect. A* **581**, 761
Takada, A. et al.: 2007, *Nucl. Instrum. Methods Phys. Res. Sect. A* **573**, 195
Tanimori, T. et al.: 2004, *Phys. Lett. B* **578**, 241
Y Takeuchi and others: 1999, *Phy. Lett. B* **452**, 418